Supporting Information

Single microcrystals of organoplatinum(II) complexes with high charge-carrier mobility

Chi-Ming Che,*[a] Cheuk-Fai Chow,[a] Mai-Yan Yuen,[a] V. A. L. Roy,[ab] Wei Lu,[a] Yong Chen,[a] Stephen Sin-Yin Chui[a] and Nianyong Zhu[a]

[a] *Department of Chemistry, Institute of Molecular Functional Materials, and HKU-CAS Joint Laboratory on New Materials, The University of Hong Kong, Pokfulam Road, Hong Kong SAR, China. E-mail: cmche@hku.hk*

[b] *Current address: Department of Physics and Materials Science, City University of Hong Kong, Tat Chee Avenue, Kowloon, Hong KongSAR, China.*

Experimental Section

All starting materials were purchased from commercial sources and used as received. The solvents used for synthesis were of analytical grade unless stated otherwise. The solvents used for nanostructure preparations and photophysical measurements were of HPLC grade. The compounds, 2,6-bis-(1*H*-pyrazol-3-yl)pyridine (**H_2L^1**),[1] 6-(1*H*-pyrazol-3-yl)-2,2-bipyridine (**HL^5**),[2] and 2,6-bis-(1*H*-imidazol-2-yl)pyridine (**H_2L^6**),[3] were prepared according to literature methods. The synthetic route for **HL^4** is depicted in Scheme S1.

Electrospray (ESI) mass spectra were measured with a PE SCIEX API 365 LC-MS/MS system. ^{1}H NMR spectra were recorded with Bruker DRX 300 or Avance 400 FT-NMR spectrometers. Elemental analyses were performed by Beijing Institute of Chemistry, Chinese Academy of Sciences. Infrared spectra were recorded on a Bio-Rad FT-IR spectrometer. UV-vis absorption spectra were recorded on a Perkin-Elmer Lambda 19 UV/vis spectrophotometer. Emission spectra were measured on a Spex Fluorolog-3 spectrofluorometer. Emission lifetimes were measured with a Quanta Ray DCR-3 pulsed Nd:YAG laser system (pulse output 355 nm, 8 ns). Luminescent quantum yields were referenced to degassed $[Ru(bpy)_3](ClO_4)_2$ in acetonitrile ($\Phi_r = 0.062$) with an estimated error of ±15%.

TEM and SAED were performed on a Philips Tecnai G2 20 S-TWIN transmission electron microscope with an accelerating voltage of 200 kV. The

[1] Y.-I. Lin, S. A. Jr. Lang, *J. Heterocycl. Chem.* **1977**, *14*, 345–347.

[2] J. S. Fleming, E. Psillakis, S. M. Couchman, J. C. Jeffery, J. A. McCleverty, M. D. Ward, *J. Chem. Soc., Dalton Trans.* **1998**, 537–543

[3] M. E. Voss, C. M. Beer, S. A. Mitchell, P. A. Blomgren, P. E. Zhichkin, *Tetrahedron* **2008**, *54*, 645–651.

TEM images and SAED patterns were taken by Gatan MultiScan Camera Model 794. TEM samples were prepared by depositing a few drops of suspensions on the formvar-coated copper grids and the excess solvent was removed by a piece of filter paper. The SEM images were taken on a Hitachi S-4800 field emission scanning electron microscope operating at 3.0 kV. SEM samples were prepared by drop-casting suspensions onto silicon wafers. Gold sputtering was applied before SEM observations.

The X-ray diffraction data of **1a**·$(CH_3OH)_2$, **3a**·$(H_2O)_{0.67}$, and **3b** were collected on a MAR diffractometer using Mo-Kα radiation (λ = 0.71073 Å). The X-ray diffraction data of **6**·(DMSO)·$(H_2O)_2$ was collected on a Bruker AXS Proteum X8 diffractrometer using Cu-Kα radiation (λ = 1.54056 Å). The crystal structures were solved (SHELXS-97) by direct methods and refined (SHELXL-97) by full-matrix least-square on F^2. All non-H atoms were refined anisotropically.

A common substrate-gate structure field effect transistor (FET) was fabricated. The SiO_2 layer (100 nm, relative permittivity = 3.9), heavily doped n-type Si substrates, Ti adhesion film (10 nm, lower)/Au conductive film (50 nm, upper) were used as the insulator, gate electrode and source/drain electrodes, respectively. The transistor channel length in between the two electrodes is 5 μm. A drop of the suspension of organoplatinum(II) microcrystals was drop-cast onto the top of the bottom contact devices and dried in air. The output and transfer characteristics and photoresponsive transient measurements were performed on an Agilent 4155C Semiconductor Parameter Analyzer at room temperature in air and in an electrically-shielded condition. Since the saturation of the drain current was

not attained, the charge-carrier mobility (μ) was calculated from the linear regime using $I_{D,lin}$ vs. V_G relation.[4] At the linear regime where $V_{DS} << V_{GS}$,

$$\mu = \frac{L}{W C_{ox} V_{DS}} \frac{\partial I_{DS}}{\partial V_{GS}}$$

(where W is the channel width; L is the channel length; C_{ox} is the capacitance of the SiO_2 insulating layer; V_{GS} is the gate voltage, V_{DS} is the drain-source voltage and I_{DS} is the channel (drain-source current).

[4] S. M. Sze, *Physics of Semiconductor Device, 2nd ed.*; Wiley: New York, US, 1981.

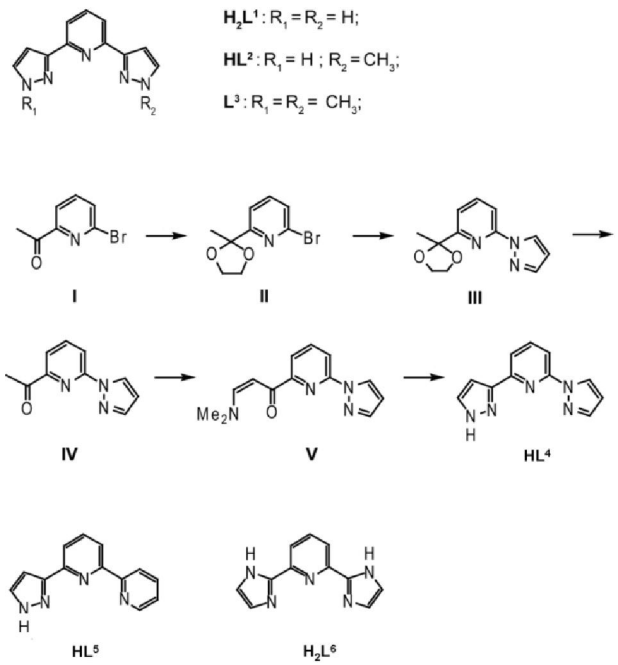

Scheme S1 Chemical Structures of ligands $HL^{1–6}$ and the synthesis of HL^4.

2-(1*H*-pyrazol-3-yl)-6-(1-*methyl*-pyrazol-3-yl)pyridine (HL^2):

A mixture of $\mathbf{H_2L^1}$ (0.211 g, 1.0 mmol), iodomethane (0.142 g, 1.0 mmol) and Na_2CO_3 (0.106 g, 1.0 mmol) in DMF was refluxed under N_2 atmosphere for 24 hours. After removal of solvent in vacuo, the resultant solid was purified by flash chromatography on Al_2O_3 eluting with $CHCl_3$, affording $\mathbf{HL^2}$ as a white solid. Yield: 0.15 g, 65%. ^{1}H NMR (400 MHz, *$CDCl_3$*) δ 3.95 (s, 3H), 6.79 (s, 1H), 6.88 (d, *J* = 2.0 Hz, 1H), 7.38 (d, *J* = 2.2, 1H), 7.59 (d, *J* = 7.4, 1H), 7.65 (d, *J* = 1.5, 1H), 7.72 (t, *J* = 7.7, 1H), 7.81 (d, *J* = 7.8, 1H). ESI-MS (+ve m/z): 226.2 $[M+H]^+$.

2,6-Di(1-*methyl*-pyrazol-3-yl)pyridine (L^3):

A mixture of $\mathbf{H_2L^1}$ (0.211 g, 1.0 mmol), 1-iodomethane (0.284 g, 2.0 mmol) and CH_3ONa (0.108 g, 2.0 mmol) in anhydrous THF was refluxed under nitrogen

atmosphere for 12 hours. The mixture was cooled at room temperature. After removal of solvent in vacuo, a pale yellow solid was obtained. The crude product was purified by flash chromatography on Al_2O_3 with $CHCl_3$ as eluent, giving **L**[3] as a white solid. Yield: 0.28 g, 85%. ^{1}H NMR (400 MHz, *CDCl*$_3$) δ 3.98 (s, 6H), 7.00 (d, *J* = 2.1 Hz, 2H), 7.41 (d, *J* = 2.1 Hz, 2H), 7.74 (t, *J* = 7.3 Hz, 1H), 7.84 (d, *J* = 7.7 Hz, 2H). ESI-MS (+ve m/z): 240.1 $[M+H]^+$.

2-(1*H*-Pyrazol-3-yl)-6-(2*N*-pyrazolyl)pyridine (HL[4]):

The synthesis of **HL**[4] involves a 5-step process described below.

(i) 6-bromo-2-(2-methyl-1,3-dioxolan-2-yl)-pyridine, (II).

This was prepared according to a literature procedure.[5]

(ii) 2-(2-methyl-1,3-dioxolan-2-yl)-6-(2*N*-pyrazolyl)pyridine, (III).

To a suspension of NaH (60% dispersion in mineral oil, 1.0 g, 0.025 mol) in anhydrous DMF (20 mL) under a nitrogen atmosphere was added dropwise a solution of pyrazole (1.68 g, 0.025 mol) in anhydrous DMF (30 mL). After 1 h, compound **II** (2.0 g, 0.01 mol) was added dropwise, and the mixture was stirred at 80 °C for 12 hours. Ice water was added to the reaction mixture, which was subsequently extracted with ethylacetate. The combined extracts were washed with water and brine, dried, and filtered, and the solvent was removed under vacuum. The product was purified by flash chromatography (DCM-hexane 2/3) to give compound **III** as a pale yellow oil. Yield: 1.74 g, 75%. ^{1}H NMR (400 MHz, *CDCl*$_3$) δ1.87 (s, 3H), 4.04 (m, 2H), 4.20 (m, 2H), 6.52 (t, *J* = 2.57 Hz, 1H), 7.51

[5] C. Bianchini, G. Giambastiani, I. G. Rios, A. Meli, W. Oberhauser, L. Sorace, A. Toti, *Organometallics* **2007**, *26*, 5066–5078.

(d, J = 8.15 Hz, 1H), 7.80 (d, J =2.50 Hz, 1H), 7.89 (t, J = 8.15 Hz, 1H), 8.00 (d, J = 8.18 Hz, 1H), 8.72 (d, J = 2.58 Hz, 1H). ESI-MS (+ve m/z): 232.2 $[M+H]^+$.

(iii) 2-acetyl-6-(2*N*-pyrazolyl)pyridine, (IV).

A mixture of **III** (1 g, 4.32 mmol), acetone (25 mL) and HCl (10 mL, 2M) was stirred in room temperature for 12 hours. The mixture was concentrated and neutralized with a saturated $NaHCO_3$ solution. The solution was extracted with CH_2Cl_2 and the organic phase was collected, washed with saturated $NaHCO_3$ and brine, dried over $MgSO_4$, and evaporated to give a pale yellow oil as crude product. The crude product was purified with chromatography on silica gel, eluting with (DCM-hexane 1/1.5), and affording **IV** as a white solid. Yield: 0.79g, 98%. ^{1}H NMR (400 MHz, *CDCl*$_3$) δ 2.84 (s, 3H), 6.59 (t, J = 2.12 Hz, 1H), 7.84 (d, J =2.02 Hz, 1H), 8.00 (m, 2H), 8.26 (d, J = 7.83 Hz, 1H), 8.71 (d, J = 2.61 Hz, 1H). ESI-MS (+ve m/z): 187.3 $[M+H]^+$.

(iv) 3-Dimethylamino-1-[6-(2*N*-pyrazolylpyridine-2-yl)-propenone, (V).

A mixture of **IV** (0.5 g, 2.68 mmol) and *N*,*N*-dimethylformamide dimethyl acetal (5 ml) was heated to reflux with stirring under N_2 for 16 hours. During the course of the reaction, the reaction mixture changed from colorless to orange. The reaction mixture was concentrated under vacuum. *n*-Hexane was added to the mixture to give an orange solid (100%), which was collected without any purification. ^{1}H-NMR (400 MHz, *CDCl*$_3$) δ ppm 8.67 (d, J = 2.52 Hz, 1H), 8.07 (t, J = 7.04 Hz, 2H), 7.93 (m, 2H), 7.70 (d, J =1.90 Hz, 1H), 6.53 (m, 2H), 3.22 (s, 3H), 3.13 (s, 3H). ESI-MS (+ve mode): m/z 243.3 $[M+H]^+$.

(v) 2-(1*H*-pyrazol-3-yl)-6-(2*N*-pyrazolyl)pyridine, **HL^4**.

A mixture of **V** (0.5 g, 2.06 mmol) and hydrazine monohydrate (0.31 g, 6.18 mmol) in EtOH (10 mL) was refluxed for 2 hours. A pale yellow solid was

obtained by removal of solvent. Further washing with diethyl ether gave the pure product as white solid. Yield: 0.39 g, 89%. ^{1}H-NMR (400 MHz, *CDCl$_3$*) δ6.50 (t, *J* = 2.00 Hz, 1H), 6.88 (d, *J* = 2.00 Hz, 1H), 7.82-7.62 (m, 3H), 7.97-7.83 (m, 2H), 8.65 (d, *J* = 2.60 Hz, 1H). ESI-MS (+ve m/z): 212.3 $[M+H]^+$.

The platinum (II) complexes were obtained by refluxing *cis*-$[Pt(DMSO)_2Cl_2]$ with the corresponding ligands in acidified methanolic solutions for 3–18 hours under an nitrogen atmosphere. The complexes were obtained as a chloride salt. The perchlorate salts (ClO_4^-) were obtained by metathesis reaction of corresponding chloride salts.

[Pt(H$_2$L^1)Cl]Cl (1a):

cis-$[Pt(DMSO)_2Cl_2]$ (0.422 g, 1.0 mmol), **H$_2$L^1** (0.211 g, 1.0 mmol) and hydrochloric acid (0.1 g, 1.0 mmol) were dissolved in MeOH (200 mL) and refluxed for 3 hours under nitrogen atmosphere. A yellow precipitate was obtained. Yellow crystals were obtained by slow evaporation of a methanolic solution of the crude product. Yield: 0.46g, 97%. ^{1}H-NMR (400 MHz, CD_3OD) δ 7.18 (s, 2H), 7.95 (broad s, 2H), 8.04 (s, 2H), 8.24 (broad s, 1H). ESI-MS (+ve m/z): 441.1 [**M**]$^+$. Elemental analyses for $C_{11}H_9Cl_2N_5Pt{\cdot}2CH_3OH$, Calc.: C, 31.64; H, 3.72; N, 12.45. Found: C, 31.58; H, 3.74; N, 12.48. IR (KBr): *ν* 3117 cm^{-1}(C–H), 3417 cm^{-1} (N–H).

[Pt(H$_2$L^1)Cl]ClO$_4$ (1b):

A mixture of **1a** (0.119 g, 0.25 mmol) and $LiClO_4$ (0.05 g, 2.5 mmol) in methanol (50 mL) was stirred at room temperature for 12 hours. A yellow solid

was obtained by slow vapor diffusion of diethyl ether into a methanol solution. Elemental analyses for $C_{11}H_9Cl_2N_5O_4Pt{\cdot}CH_3OH$, Calc.: C, 26.59; H, 2.57; N, 11.93. Found: C, 26.32; H, 2.44; N, 12.05. IR (KBr): *v* 3124 cm^{-1}(C–H), 3440 cm^{-1} (N–H).

[Pt(HL^2)Cl]Cl (2a):

cis-[Pt(DMSO)$_2$Cl$_2$] (0.211 g, 0.5 mmol), **HL^2** (0.5 mmol) and hydrochloric acid (0.5 mmol) were dissolved in MeOH/$CHCl_3$ (v/v 1:1, 100 ml) mixture. The reaction mixture was refluxed for 18 hours under nitrogen atmosphere. Upon removal of solvent, a yellow solid was obtained and was washed with diethyl ether. A yellow crystalline powder was obtained by slow evaporation of methanol solution. Yield: 0.24 g, 97 %. ^{1}H NMR (400 MHz, *MeOD*) δ 4.09 (s, 3H), 7.01 (d, *J* = 2.8 Hz, 1H), 7.14 (d, *J* = 2.9 Hz, 1H), 7,82 (t, 2H), 8.02 (d, *J* = 2.8, 1H), 8.04 (d, *J* = 2.9, 1H), 8.20 (t, *J* = 8.0 Hz, 1H). ESI-MS (+ve m/z): 455.1 [**M**]$^+$. Elemental analyses for $C_{12}H_{11}Cl_2N_5Pt$, Calc.: C, 29.34; H, 2.26; N, 14.26. Found: C, 29.19; H, 2.33; N, 14.14. IR (KBr): *v* 3101 cm^{-1}(C–H), 3409 cm^{-1} (N–H).

[Pt(HL^2)Cl]ClO_4 (2b):

A mixture of **2a** (0.25 mmol) and $LiClO_4$ (0.05 g, 2.5 mmol) in acetonitrile (50 mL) was stirred for 12 hours at room temperature. A yellow solid was obtained by slow vapor diffusion of diethyl ether into an acetonitrile solution. Elemental analyses for $C_{12}H_{11}Cl_2N_5O_4Pt{\cdot}CH_3CN$, Calc.: C, 28.20; H, 2.37; N, 14.09. Found: C, 28.09; H, 2.22; N, 14.14. IR (KBr): *v* 3109 cm^{-1}(C–H), 3394 cm^{-1} (N–H).

[Pt(L^3)Cl]Cl (3a):

A mixture of *cis*-[Pt(DMSO)$_2$Cl$_2$] (0.211 g, 0.5 mmol) and **L^3** (0.120 g, 0.5 mmol) in MeOH (50 mL) was refluxed for 18 hours under nitrogen atmosphere to give a clear yellow solution. A yellow solid was obtained after removal of solvent and was washed diethyl ether. Yield: 0.24 g 97 %. ^{1}H-NMR (400 MHz, *DMSO*) δ 4.13 (s, 6H), 7.38 (d, *J* = 2.7 Hz, 2H), 8.16 (d, *J* = 8.0 Hz, 2H), 8.28 (d, *J* = 2.7 Hz, 2H), 8.41 (t, *J* = 8.0 Hz, 1H). ESI-MS (+ve m/z): 469.5 [**M**]$^+$. Elemental analyses for $C_{13}H_{13}Cl_2N_5Pt{\cdot}2CH_3OH$, Calc.: C, 31.64; H, 3.72; N, 12.30. Found: C, 31.81; H, 3.88; N, 12.11. IR (KBr): *v* 3110 cm^{-1}(C–H).

[Pt(L^3)Cl]ClO$_4$ (3b):

A mixture of **3a** (0.25 mmol) and $LiClO_4$ (0.05 g, 2.5 mmol) was stirred in methanol (50 mL) for 24 hours at room temperature. Yellow crystals were obtained by slow vapor diffusion of diethyl ether into a chloroform solution of **3b**. Elemental analyses for $C_{13}H_{13}Cl_2N_5O_4Pt{\cdot}CHCl_3$, Calc.: C, 24.42; H, 2.05; N, 10.17. Found: C, 24.21; H, 2.06; N, 10.22. IR (KBr): *v* 3113 cm^{-1}.

[Pt(HL^4)Cl]Cl (4):

A mixture of *cis*-[Pt(DMSO)$_2$Cl$_2$] (0.422 g, 1.0 mmol), **HL^4** (0.211 g, 1.0 mmol) and hydrochloric acid (1.0 mmol) in MeOH (200 mL) was refluxed for 18 hours under an inert atmosphere to give a yellow suspension. The yellow solid was collected and washed with diethyl ether. Yield: 0.39 g, 81 %. ^{1}H NMR (400 MHz, MeOD) δ 6.08 (t, *J* = 2.0 Hz, 1H), 6.53 (m, 2H), 7.00-7.40 (m, 2H), 7.50-7.70 (m, 1H), 7.80-8.10 (m, 1H), 8.39 (d, *J* = 2.0 Hz, 1H). ESI-MS (+ve m/z): 441.0 [**M**]$^+$. Elemental analyses for $C_{11}H_9Cl_2N_5Pt{\cdot}H_2O$, Calc.: C, 26.68; H, 2.24;

N, 14.14. Found: C, 26.57; H, 2.11; N, 14.15. IR (KBr): *v* 3078 cm^{-1}(C–H), 3402 cm^{-1} (N–H).

[Pt(HL^5)Cl]Cl (5):

A mixture of *cis*-[Pt(DMSO)$_2$Cl$_2$] (0.422 g, 1.0 mmol), **HL^5** (0.222 g, 1.0 mmol) and hydrochloric acid (1.0 mmol) in MeOH (200 mL) was refluxed for 12 hours under an inert atmosphere to give a yellow suspension. A yellow solid was filtered, washed with methanol, diethyl ether and dried under vacuum. Yield 0.25 g, 51 %. ^{1}H NMR (400 MHz, *d-DMSO*) δ 7.14-7.20 (m, 1H), 8.02-8.10 (m, 1H), 8.11-8.26 (m, 2H), 8.31-8.41 (m, 3H), 8.71-8.79 (m, 1H), 8.86 (d, *J* = 8.19 Hz, 1H), 12.5 (br, 1 H). ESI-MS (+ve m/z): 452.0 [**M**]$^+$. Elemental analyses for $C_{13}H_{10}Cl_2N_4Pt{\cdot}2H_2O$, Calc.: C, 29.78; H, 2.69; N, 10.69. Found: C, 29.68; H, 2.77; N, 10.55. IR (KBr): *v* 3085 cm^{-1}(C–H), 3402 cm^{-1} (N–H).

[Pt(H$_2$L^6)Cl]Cl (6):

A mixture of *cis*-[Pt(DMSO)$_2$Cl$_2$] (0.422 g, 1.0 mmol), **H$_2$L^6** (0.211 g, 1.0 mmol) and HCl (2.0 mmol) in methanol (100 mL) was refluxed for 12 hours under nitrogen atmosphere to give a yellow orange suspension. A yellow orange solid was obtained, washed with chloroform and dried under vacuum. Yellow needle shape crystals were obtained by slow diffusion of $CHCl_3$ into DMSO solution. Yield: 0.39 g, 80 %. ^{1}H-NMR (400 MHz, *DMSO*) δ 7.87-7.99 (m, 3H), 8.06 (d, *J* = 8.08 Hz, 2H), 8.36-8.49 (m, 2H). ESI-MS (+ve m/z): 441.0 [**M**]$^+$. Elemental analyses for $C_{11}H_9Cl_2N_5Pt$, Calc.: C, 27.69; H, 1.90; N, 14.68; Found: C, 27.58; H, 1.93; N, 14.62. IR (KBr): *v* 3124 cm^{-1} (C–H), 3510 cm^{-1} (N–H).

Table S1 Crystal and Structure Determination Data.

	1·2CH_3OH	**3a**·0.67H_2O	**3b**	**6**·DMSO·2H_2O
Formula	$C_{13}H_{17}Cl_2N_5O_2Pt$	$C_{39}H_{39}Cl_6N_{15}O_2Pt_3$	$C_{13}H_{13}Cl_2N_5O_4Pt$	$C_{13}H_{19}N_5Cl_2O_3SPt$
Formula Weight	541.31	1547.79	569.26	591.38
Crystal system	Triclinic	Monoclinic	Monoclinic	Monoclinic
Space group	*P*-1	*P* $2_1/c$	*P* $2_1/c$	*P* $2_1/c$
a, Å	6.848(1)	12.588(2)	10.669(2)	9.4740(3)
b, Å	11.736(2)	18.736(3)	10.411(2)	7.1809(2)
c, Å	12.384(3)	20.805(4)	15.689(3)	27.9371(8)
α, deg	65.95(3)	90	90	90
β, deg	79.94(3)	106.39(2)	108.89(3)	91.940(1)
γ, deg	76.84(3)	90	90	90
V, $Å^3$	881.2(3)	4707.3(1)	1648.8(6)	1899.5(1)
Z	2	4	4	4
T, K	301(2)	301(2)	301(2)	173(2)
μ, mm^{-1}	8.279	9.288	8.865	17.648
Reflections collected	5150	27598	9437	3299
Unique reflection	3268	8927	3116	3123
R_{int}	0.0178	0.0524	0.0188	0.048
Observed reflections [$I > 2\alpha(I)$]	3092	5755	2956	2986
R_1	0.0205	0.0343	0.0187	0.0463
wR_2	0.0509	0.0693	0.0479	0.1200

Table S2 Selected Bond Lengths [Å] and Bond Angles [deg] for **1a** and **3a**.

1a				**3a**			
Bond Length (Å)		**Bond Angle (deg)**		**Bond Length (Å)**		**Bond Angle (deg)**	
Pt(1)-N(2)	1.987(3)	N(3)-Pt(1)-N(2)	79.57(13)	Pt(1)-N(1)	2.015(6)	N(5)-Pt(1)-N(1)	79.1(3)
Pt(1)-N(2)	1.987(3)	N(3)-Pt(1)-N(4)	79.44(14)	Pt(1)-N(5)	1.958(6)	N(5)-Pt(1)-N(3)	79.4(3)
Pt(1)-N(4)	2.003(3)	N(2)-Pt(1)-N(4)	159.02(13)	Pt(1)-N(3)	2.018(6)	N(1)-Pt(1)-N(3)	158.4(3)
Cl(1)-Pt(1)	2.2903(1)	N(3)-Pt(1)-Cl(1)	179.34(9)	Cl(1)-Pt(1)	2.289(2)	N(5)-Pt(1)-Cl(1)	179.7(2)
N(1)-H(1B)	0.8600	N(2)-Pt(1)-Cl(1)	99.77(10)	N(2)-C(1)	1.464(1)	N(1)-Pt(1)-Cl(1)	100.79(2)
N(5)-H(5A)	0.8600	N(4)-Pt(1)-Cl(1)	101.21(11)	N(4)-C(13)	1.464(1)	N(3)-Pt(1)-Cl(1)	100.75(2)
N(1)-N(2)	1.349(4)	C(3)-N(2)-Pt(1)	115.7(2)	N(2)-N(1)	1.339(8)	C(4)-N(1)-Pt(1)	114.3(5)
C(3)-N(2)	1.346(5)	N(1)-N(2)-Pt(1)	137.3(3)	C(4)-N(1)	1.345(9)	N(2)-N(1)-Pt(1)	138.3(5)
C(4)-N(3)	1.347(5)	C(8)-N(3)-Pt(1)	118.9(3)	C(5)-N(5)	1.347(1)	C(5)-N(5)-Pt(1)	118.9(5)
C(8)-N(3)	1.346(5)	C(4)-N(3)-Pt(1)	118.6(2)	C(9)-N(5)	1.361(9)	C(9)-N(5)-Pt(1)	119.3(5)
C(9)-N(4)	1.351(5)	N(5)-N(4)-Pt(1)	137.6(3)	C(10)-N(3)	1.362(1)	N(4)-N(3)-Pt(1)	139.1(5)
N(4)-N(5)	1.332(5)	C(9)-N(4)-Pt(1)	114.9(3)	N(4)-N(3)	1.348(9)	C(10)-N(3)-Pt(1)	114.1(5)

Table S3 Selected Bond Lengths [Å] and Bond Angles [deg] for **3b** and **6**.

3b				**6**			
Bond Length (Å)		**Bond Angle (deg)**		**Bond Length (Å)**		**Bond Angle (deg)**	
Pt(1)-N(1)	2.015(6)	N(5)-Pt(1)-N(1)	79.1(3)	Pt(1)-N(3)	1.95 (4)	N(3)-Pt(1)-N(4)	80.5(15)
Pt(1)-N(5)	1.958(6)	N(5)-Pt(1)-N(3)	79.4(3)	Pt(1)-N(4)	2.02(4)	N(3)-Pt(1)-N(1)	79.8(16)
Pt(1)-N(3)	2.018(6)	N(1)-Pt(1)-N(3)	158.4(3)	Pt(1)-N(1)	2.02(3)	N(4)-Pt(1)-N(1)	160.3(15)
Cl(1)-Pt(1)	2.289(2)	N(5)-Pt(1)-Cl(1)	179.7(2)	Pt(1)-Cl(1)	2.303(11)	N(3)-Pt(1)-Cl(1)	179.1(11)
N(2)-C(1)	1.464(1)	N(1)-Pt(1)-Cl(1)	100.79(2)	N(1)-C(3)	1.34(6)	N(4)-Pt(1)-Cl(1)	99.9(11)
N(4)-C(13)	1.464(1)	N(3)-Pt(1)-Cl(1)	100.75(2)	N(1)-C(1)	1.36(6)	N(1)-Pt(1)-Cl(1)	99.8(11)
N(2)-N(1)	1.339(8)	C(4)-N(1)-Pt(1)	114.3(5)	N(2)-C(3)	1.32(6)	C(3)-N(1)-C(1)	107(4)
C(4)-N(1)	1.345(9)	N(2)-N(1)-Pt(1)	138.3(5)	N(2)-C(2)	1.37(7)	C(3)-N(1)-Pt(1)	112.(3)
C(5)-N(5)	1.347(1)	C(5)-N(5)-Pt(1)	118.9(5)	N(3)-C(4)	1.34(6)	C(1)-N(1)-Pt(1)	140(3)
C(9)-N(5)	1.361(9)	C(9)-N(5)-Pt(1)	119.3(5)	N(3)-C(8)	1.36(6)	C(3)-N(2)-C(2)	107(4)
C(10)-N(3)	1.362(1)	N(4)-N(3)-Pt(1)	139.1(5)	N(4)-C(9)	1.34(6)	C(4)-N(3)-C(8)	121(3)
N(4)-N(3)	1.348(9)	C(10)-N(3)-Pt(1)	114.1(5)	N(4)-C(11)	1.37(6)	N(3)-C(8)-C(9)	109(4)

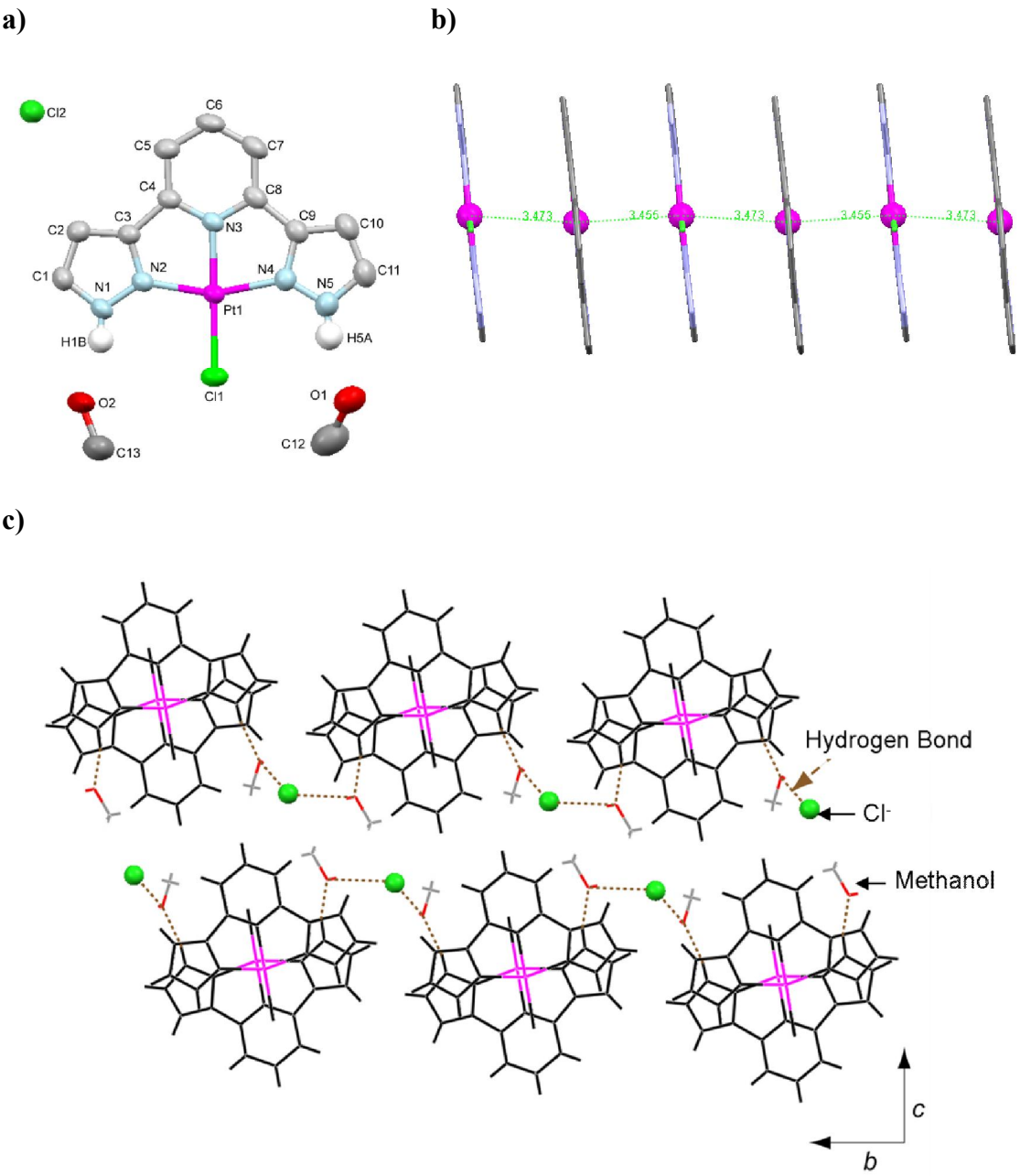

Figure S1 (a) Perspective view of $[Pt(H_2L^1)(Cl)]Cl{\cdot}2CH_3OH$ (**1a**) with numbering scheme adopted. Some hydrogen atoms are omitted for clarity. (b) Crystal packing diagram along the *c* axis showing continuous intermolecular Pt···Pt interactions. (c) H-bonding networks formed along the *b* axis. Hydrogen bonds are formed among the $N_{pyrazole}$–H, methanol molecules and chloride ion.

a)

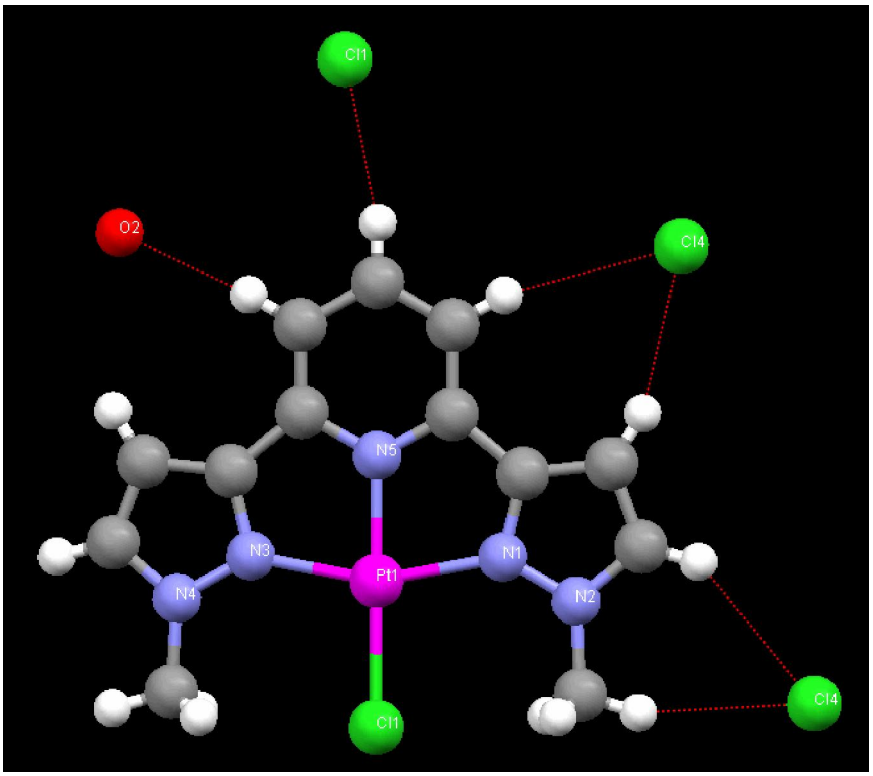

b)

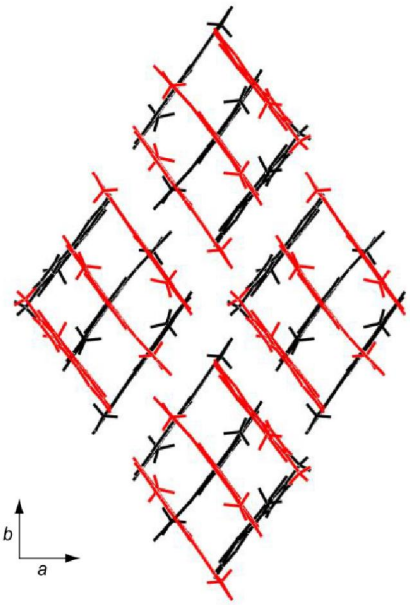

Figure S2 (a) Perspective view of [Pt(L^3)(Cl)]Cl (**3a**) with numbering scheme adopted. (b) 2-dimensional π–π interactions of the [Pt(L^3)Cl]$^+$ cations.

a)

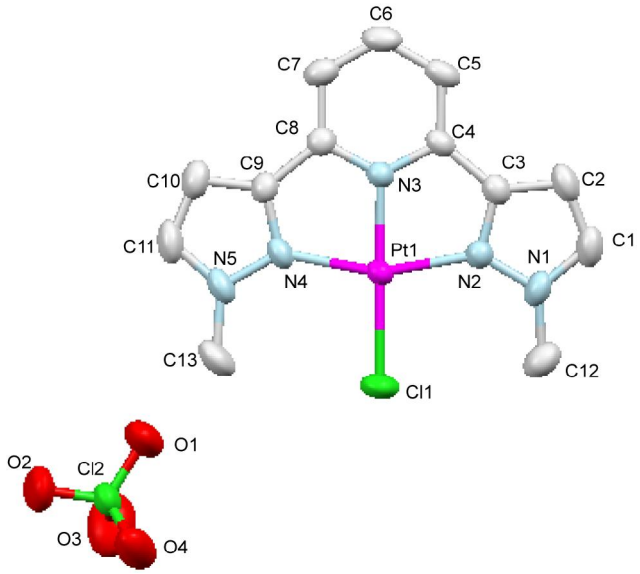

b)

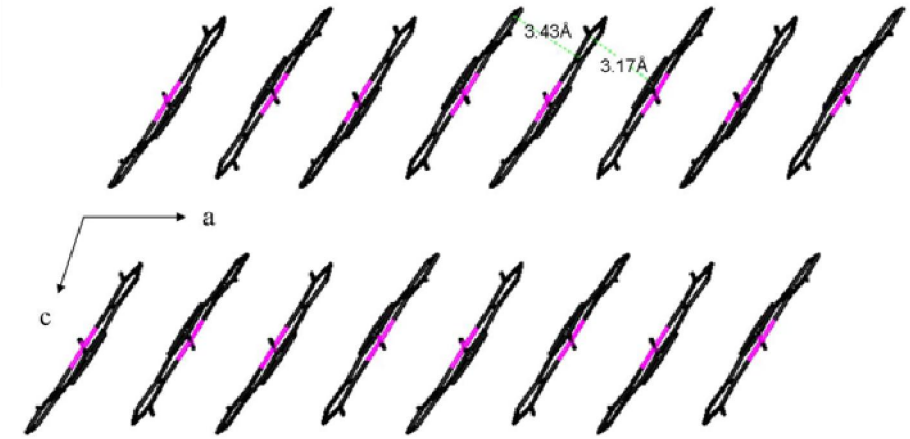

Figure S3 (a) Perspective view of $[Pt(L^3)(Cl)]ClO_4$ (**3b**) with numbering scheme adopted. (b) Continuous π–π interactions along the *a* axis with interplanar distance of 3.17 and 3.42 Å. Perchlorate anions and hydrogen atoms are omitted for clarity.

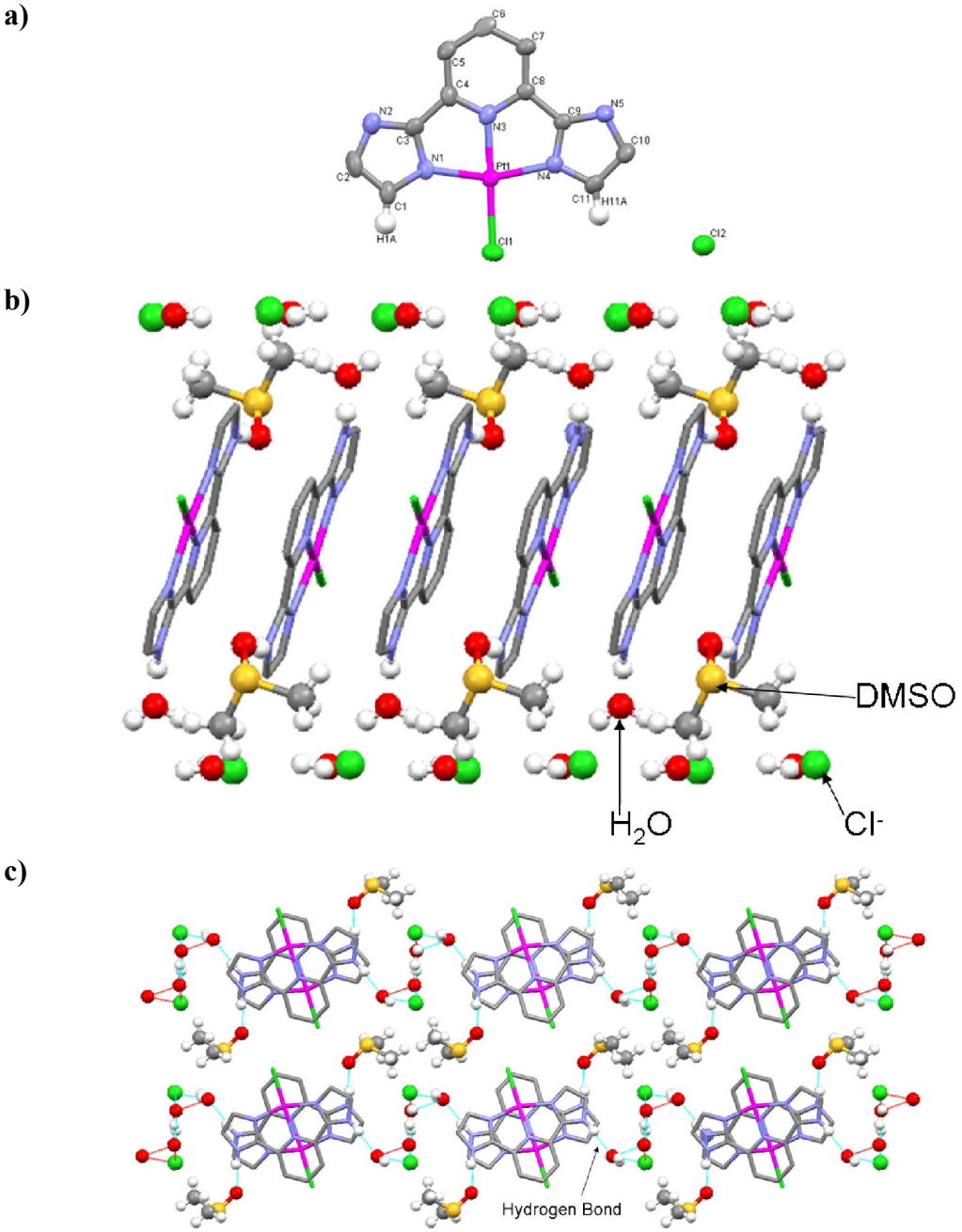

Figure S4 (a) Molecular structure of **6** with numbering scheme. (b) Dimeric stacking in head-to-tail arrangement along the *a* axis of **6** with intermolecular π–π distances of 3.370 and 3.395 Å. (c) Hydrogen bonding interaction of the **6** cations with solvent molecules (DMSO and H_2O) and chloride anion.

Table S4 Photophysical data of **1–6**

Complex	UV-vis absorption λ_{max}/nm(ε/mol^{-1} dm^{-3} cm^{-1})	Solution [a] λ_{max}/nm (τ/μs)	Quantum Yield, Φ	Solid, 298 K λ_{max}/nm (τ/μs)	Solid, 77 K λ_{max}/nm (τ/μs)	Glassy [b] λ_{max}/nm (τ/μs)
1a	258 (12600); 287 (12700); 311 (8200); 326 (7900); 342 (3500); 360 (2400); 413 (230)	491 (2.9); 523 (2.8); 565 (2.1)	6.3×10^{-2}	530 (0.2)	512 (4.3)	482 (4.8); 515 (5.5); 552 (3.7); 605 (3.5)
1b	231 (20200); 258 (17920); 275 (17350); 323 (10550); 334 (9590); 359 (3850); 418 (540)	490 (0.9)	5.8×10^{-2}	531 (0.1)	529 (4.0)	535 (8.0), 598 (4.0)
2a	267 (1459); 294 (12470); 322 (10020); 336 (9870); 365 (3270); 418 (625)	510 (0.04)	7.9×10^{-3}	542 (<0.1)	537 (0.6)	477 (2.1), 506 (2.0)
2b	237 (13710); 267 (14380); 320 (8490); 338 (8330); 361 (3330); 420 (520)	510 (3.7)	7.9×10^{-3}	567 (0.2)	567 (2.7)	551 (10.4)
3a	262 (25730); 283 (21160); 317 (13380); 328 (13520); 359 (3470); 423 (728)	505 (0.05)	3.2×10^{-3}	551 (0.3)	548 (0.6)	515 (6.8), 550 (8.7)
3b	261 (22200); 288 (18820); 314 (12910); 328 (15960); 359 (3190); 420 (720)	505 (2.9)	2.8×10^{-3}	627 (0.9)	667 (10.9)	666 (12.2)
4	281 (16345); 334 (9720); 359 (3050) 421 (365)	501 (0.05)	9.7×10^{-3}	542 (< 0.1)	554 (0.5)	466 (3.3), 499 (4.1)
5	269 (18320); 307 (9445); 340 (5110); 360 (4000); 424 (155)	554 (3.3)	2.1×10^{-3}	523 (0.3), 586 (0.2)	554 (6.0) , 602 (2.0)	518 (10.0), 557 (9.0), 602 (5.4)
6	284 (20110); 317 (17745); 349 (7715); 359 (3895); 420 (1505)	516 (9.2)	8.5×10^{-2}	Yellow form: 490 (0.4), 526 (0.4), 563 (0.3) Orange form: 620 (0.2)	505 (4.6), 541 (7.8), 617 (14.0)	483 (21.0), 528 (19.0), 570 (19.1)

[a]: Measured in degassed methanol solution [b]: Measured in glassy solution (DMF/MeOH/EtOH = v:v:v, 1:1:1) [c]: Non-emissive

Supporting Information

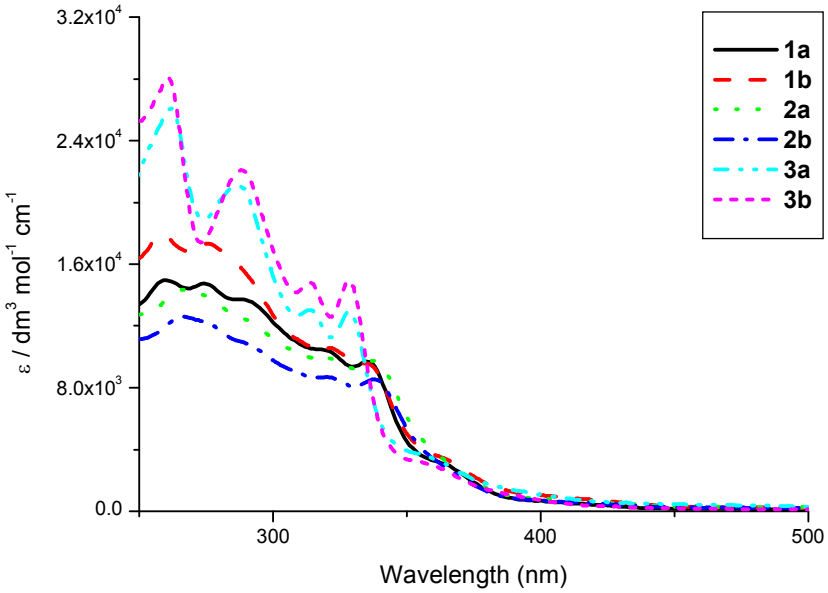

Figure S5 UV-vis absorption spectra of **1a**–**3a** in methanol at 298 K.

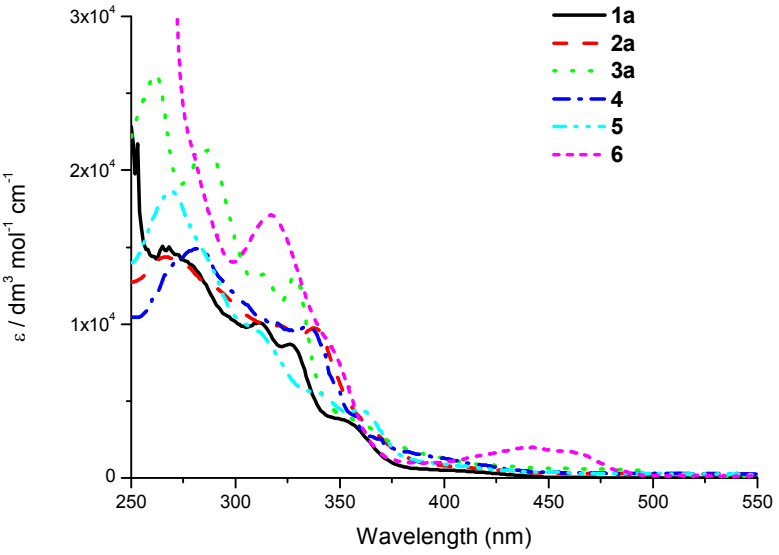

Figure S6 UV-vis absorption spectra of **1**–**5** in methanol and **6** in DMF at 298 K.

Supporting Information

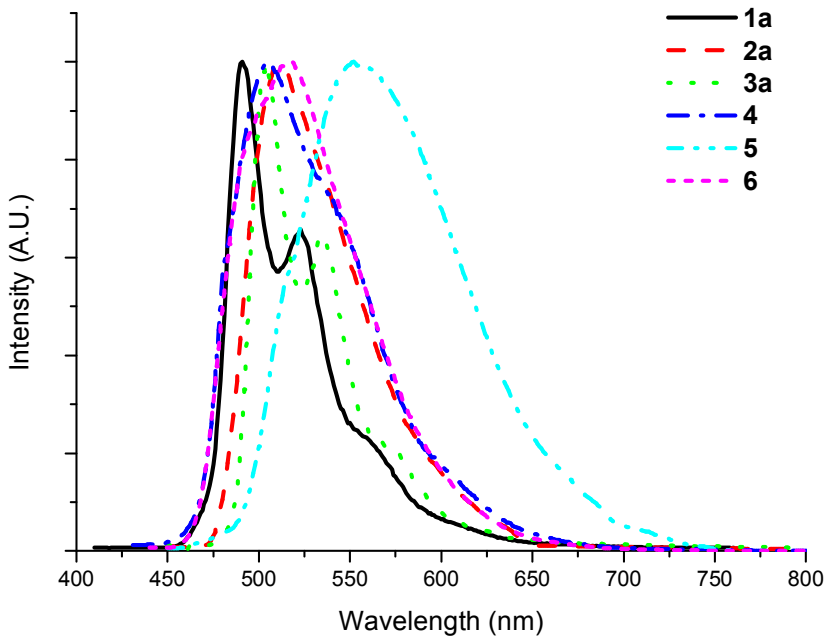

Figure S7 Emission spectra of complexes **1a**–**3a, 4**–**5** in methanol and **6** in DMF (4 x 10^{-5} mol dm^{-3}) at room temperature.

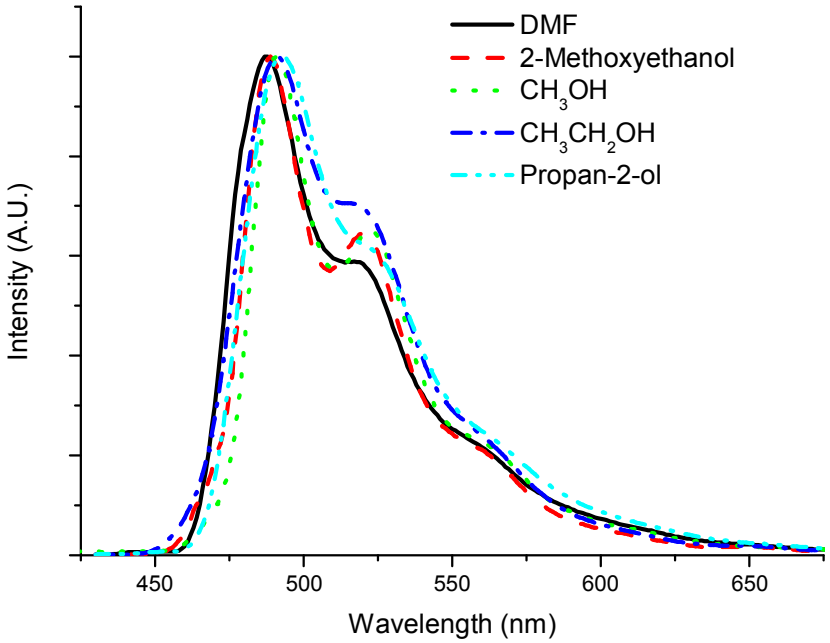

Figure S8 Emission spectra of **1a** in various solvents at 298 K.

Supporting Information

Table S5 Luminescence Data of **1a** in Various Solvents at 298 K.

Solvent	**λ_{em} [nm] (τ_0 [µs])**	**Φ**
DMF	488 (0.2); 519 (0.2); 557 (0.1)	2.5×10^{-2}
2-Methoxy-ethanol	489 (1.8); 521 (1.2); 558 (1.2)	5.8×10^{-2}
CH_3OH	491 (2.9); 523 (2.8); 565 (2.1)	6.3×10^{-2}
CH_3CH_2OH	491 (2.2); 522 (2.2); 564 (1.9)	6.2×10^{-2}
Propan-2-ol	493 (2.1); 525 (1.9); 565 (1.4)	5.4×10^{-2}

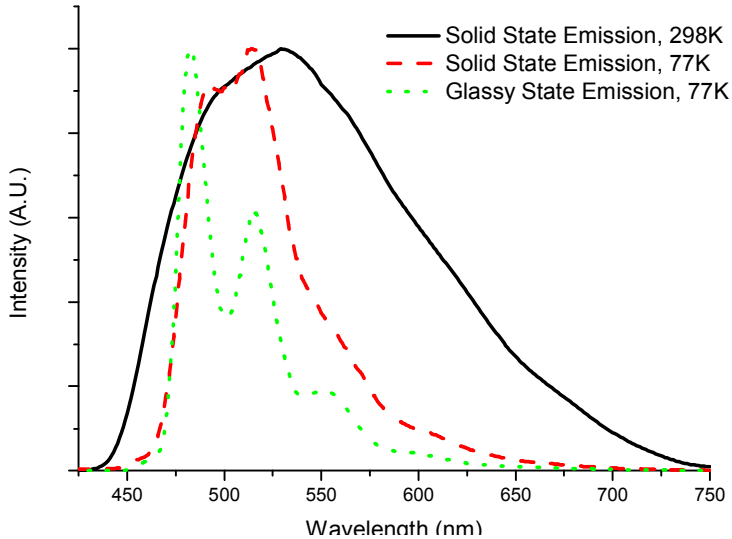

Figure S9 a) Normalized emission spectra of **1a** in solid state at 298 K, b) 77 K and c) glassy solution (1:4 MeOH/EtOH) at 77 K.

Supporting Information

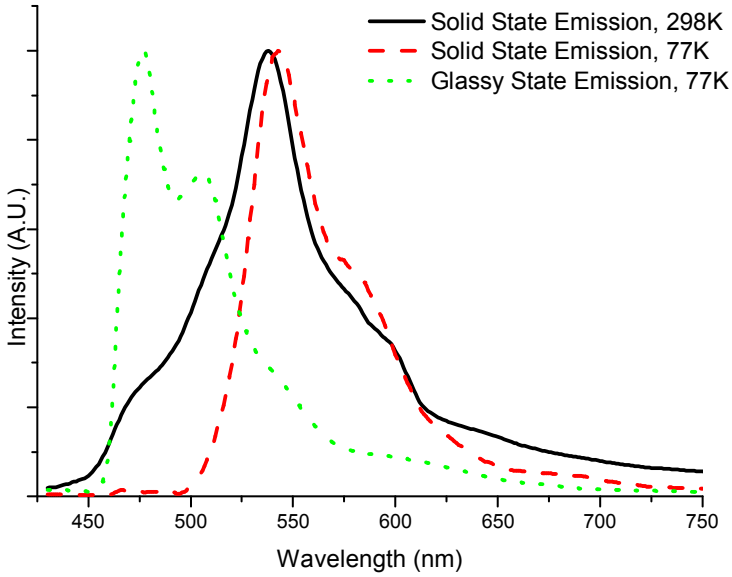

Figure S10 a) Normalized emission spectra of **2a** in solid state at 298 K, b) 77 K and c) glassy solution (1:4 MeOH/EtOH) at 77 K.

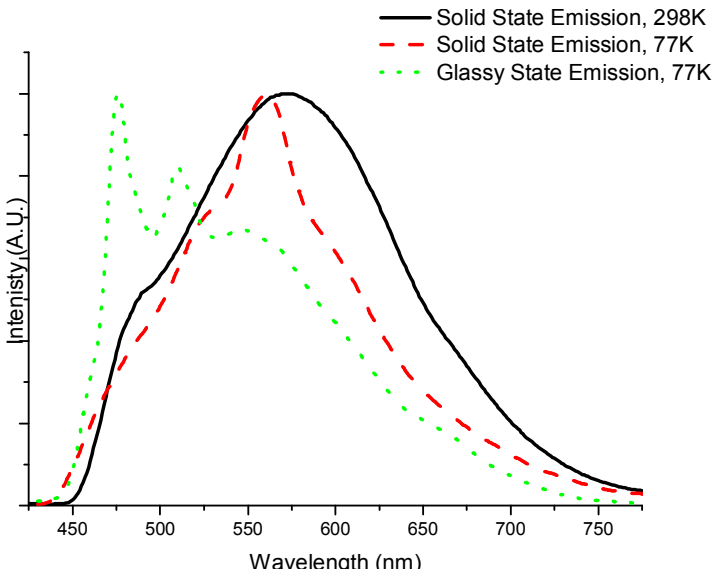

Figure S11 a) Normalized emission spectra of **3a** in solid state at 298 K, b) 77 K and c) glassy solution (1:4 MeOH/EtOH) at 77 K.

Supporting Information

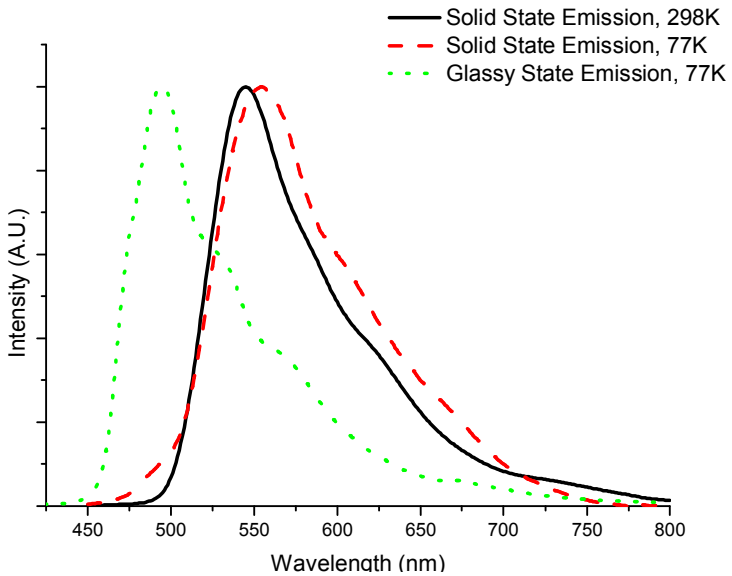

Figure S12 a) Normalized emission spectra of **4** in solid state at 298 K, b) 77 K and c) glassy solution (1:4 MeOH/EtOH) at 77 K.

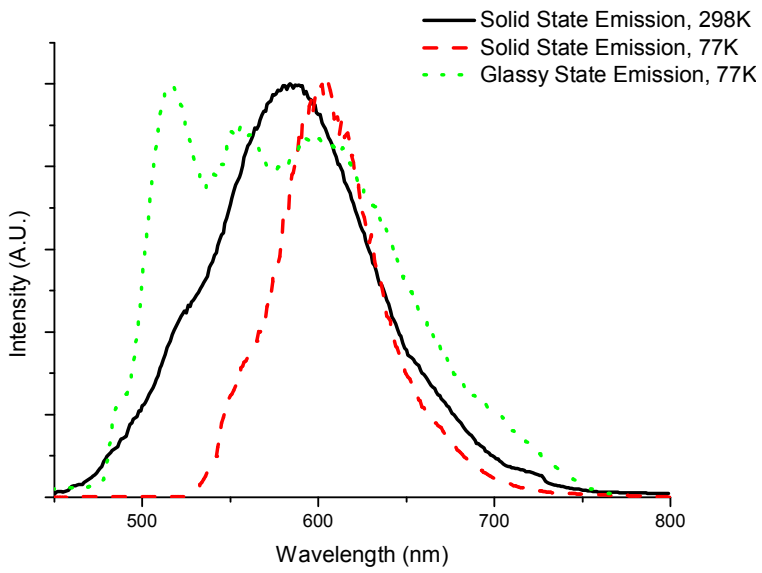

Figure S13 a) Normalized emission spectra of **5** in solid state at 298 K, b) 77 K and c) glassy solution (1:4 MeOH/EtOH) at 77 K.

Supporting Information

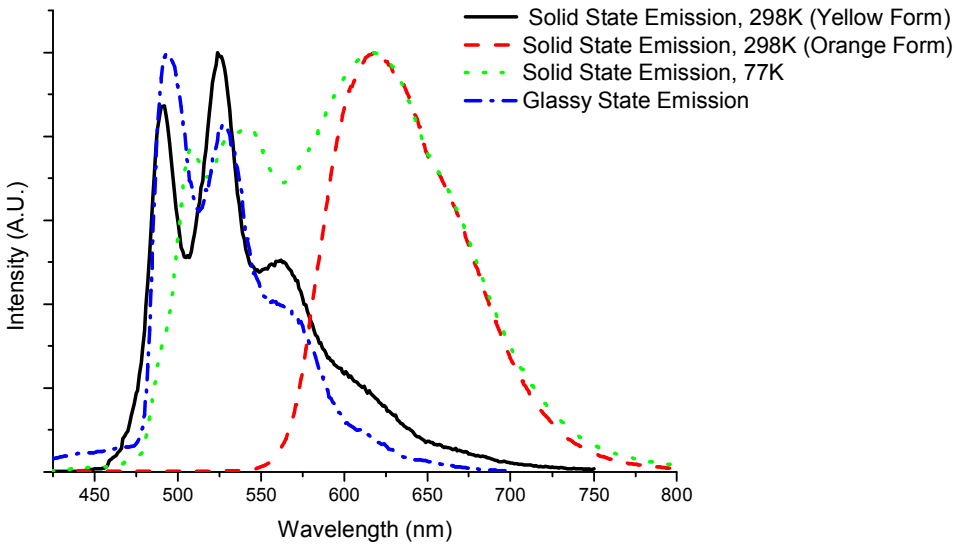

Figure S14 a) Normalized emission spectra of **6** in solid state at 298 K, b) 77 K and c) glassy solution (1:1:4 DMF/MeOH/EtOH) at 77 K.

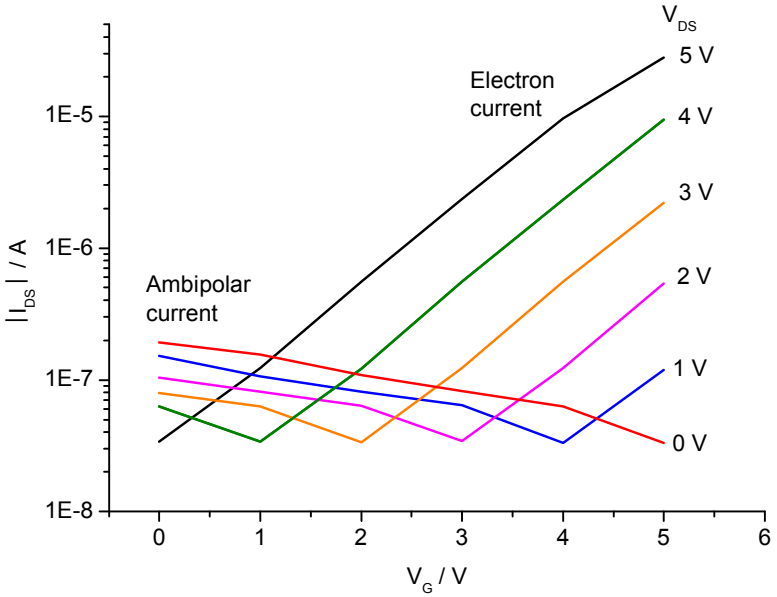

Figure S15 Transfer characteristics ($\log|I_{SD}|$ versus V_G at V_{SD}) of the single-crystal field-effect transistor of **1a**. For increasing drain-source voltages, the minimum in drain current shifts towards larger gate voltages.

Supporting Information

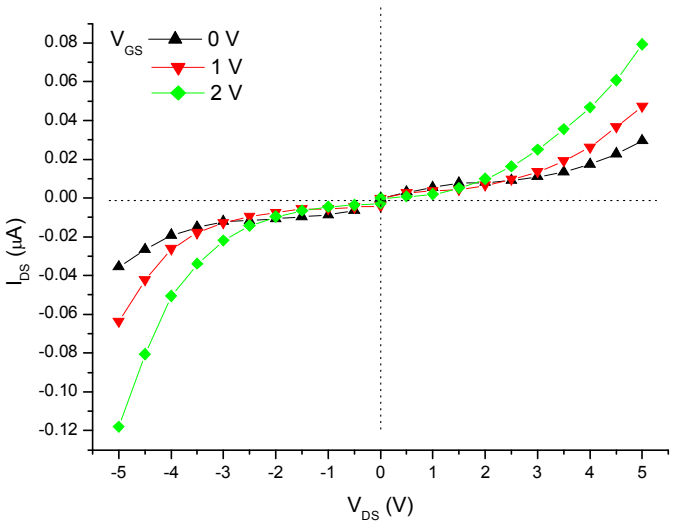

Figure S16 Output characteristics (I_{SD} versus V_{SD} at V_G) of the single-crystal field- effect transistor of **3a**.

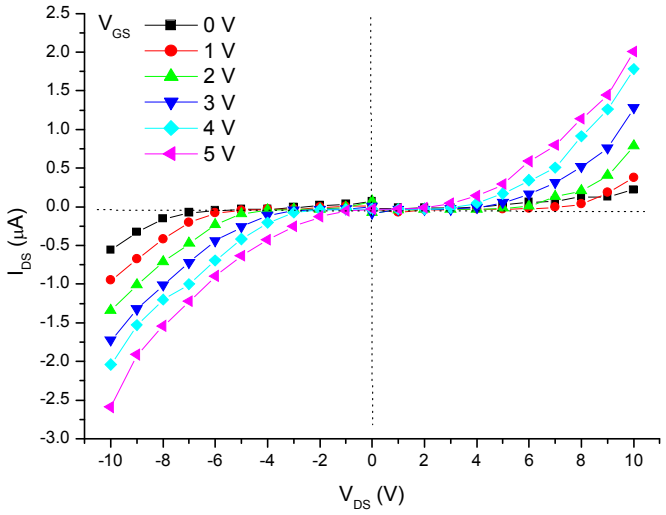

Figure S17 Output characteristics (I_{SD} versus V_{SD} at V_G) of the single-crystal field- effect transistor of **3b**.

Supporting Information

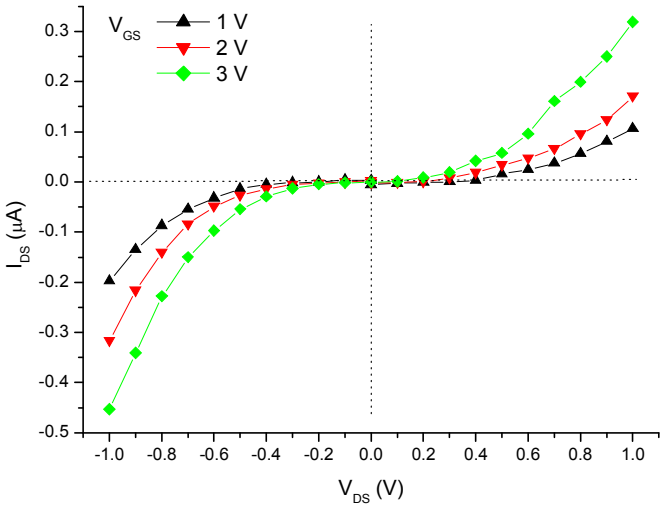

Figure S18 Output characteristics (I_{SD} versus V_{SD} at V_G) of the single-crystal field-effect transistor of **6**.